A multi-platform inversion estimation of statewide and regional methane emissions in California during 2014-2016

Yu Yan Cui[1,*], Abhilash Vijayan[1], Matthias Falk[1], Ying-Kuang Hsu[1], Dazhong Yin[1], Xue Meng Chen[1], Zhan Zhao[1], Jeremy Avise[1,2], , Yanju Chen[1], Kristal Verhulst[3], Riley Duren[3], Vineet Yadav[3], Charles Miller[3], Ray Weiss[4], Ralph Keeling[4], Jooil Kim[4], Laura T. Iraci[5], Tomoaki Tanaka[5,6], Matthew S. Johnson[5], Eric A. Kort[7], Laura Bianco[8,9], Marc L. Fischer[10], Kenneth Stroud[1], Jorn Herner[1], Bart Croes[1]

1. California Air Resources Board, 1001 I Street, Sacramento, California, USA
2. Department of Civil and Environmental Engineering, Washington State University, Pullman, Washington, USA
3. NASA Jet Propulsion Laboratory, California Institute of Technology, Pasadena, California, USA
4. Scripps Institution of Oceanography, University of California, San Diego, La Jolla, California, USA
5. Earth Science Division, NASA Ames Research Center, Moffett Field, California, USA
6. Japan Weather Association, Tokyo, Japan
7. Department of Physics, University of Michigan, Ann Arbor, Michigan, USA
8. Physical Sciences Division, NOAA Earth System Research Laboratory, Boulder, Colorado, USA
9. The Cooperative Institute for Research in Environmental Sciences, University of Colorado Boulder, Boulder, Colorado, USA
10. Lawrence Berkeley National Laboratory, Berkeley, California, USA

*Corresponding author contact information:

Yuyan Cui
California Air Resources Board/Research Division
1001 I Street, Sacramento,95814
(O) (916)3232999
Yuyan.Cui@arb.ca.gov

Revised for publication in:
Environment Science and Technology
June 13, 2019

Abstract

California methane (CH_4) emissions are quantified for three years from two tower networks and one aircraft campaign. We used backward trajectory simulations and a mesoscale Bayesian inverse model, initialized by three inventories, to achieve the emission quantification. Results show total statewide CH_4 emissions of 2.05±0.26 (at 95% confidence) Tg/yr, which is 1.14 to 1.47 times greater than the anthropogenic emission estimates by California Air Resource Board (CARB). Some of differences could be biogenic emissions, super-emitter point sources, and other episodic emissions which may not be completely included in the CARB inventory. San Joaquin Valley (SJV) has the largest CH_4 emissions (0.94±0.18 Tg/yr), followed by the South Coast Air Basin, the Sacramento Valley, and the San Francisco Bay Area, 0.39±0.18, 0.21±0.04, and 0.16±0.05 Tg/yr, respectively. The dairy and oil/gas production sources in the SJV contribute 0.44±0.36 and 0.22±0.23 Tg CH_4/yr, respectively.

Introduction

California adopted the landmark Global Warming Solutions Act of 2006 to reduce greenhouse gas emissions to the 1990 levels by 2020, and has also enacted several ambitious climate strategies to mitigate the global warming impacts of methane (CH_4), such as Senate Bill No. 1383 which requires a 40% reduction in CH_4 emissions below 2013 levels by 2030. A thorough understanding of CH_4 emission sources is critical to achieve these ambitious emission reduction goals as well as to implement efficient and cost-effective policies that will achieve real reductions.

Over the years, researchers have utilized several measurement frameworks, coupled with top-down emission estimation approaches using atmospheric measurements of CH_4 mixing ratios to quantify methane emissions in California and evaluate bottom-up inventories. These top-down studies have

included measurement and analysis schemes such as satellite and airborne remote sensing, ambient measurements and inverse modeling, source apportionment, enhancement ratios analysis[1-8]. The top-down studies for statewide CH_4 emissions from 2007 to 2014 are summarized in Table S1, and the derived total statewide emissions have ranged from 1.2-2.3 times higher than the CARB anthropogenic inventory. Similarly, top-down studies have been used to estimate CH_4 emissions in sub-regions of California (Table S2), which contain the largest methane sources in the state, including the South Coast Air Basin (SoCAB), the San Joaquin Valley (SJV), the San Francisco Bay Area (SFBA), and the Sacramento Valley (SV). The SoCAB and SFBA represent the significant urban regions and the SV contains both urban and agricultural sources. The SJV, on the other hand, is predominantly covered by agriculture activities and oil and gas production.

Most of current top-down studies rely on data from a single measurement platform. Each platform has its own advantages and limitations in constraining emissions. For instance, aircraft and satellite platforms have good spatial coverage, but aircraft platform deployment is restricted by expensive flight time and is limited to a few days a year, rendering the results as essentially daily snapshots. Similarly, most satellites provide only a once-a-day measurement window, and even the satellites that have better temporal resolution are still limited in spatial resolution and the precision necessary to resolve sources in complicated source domains, such as the SJV. Long-term tower measurements have traditionally played an important role in constraining regional emissions. However, these networks are generally expensive to site, expand, and operate, which renders a dense implementation impractical. Therefore, applying a multi-modal data platform could be a useful approach to obtain more comprehensive information about spatial and temporal resolution of emission sources in a region. Additionally, analysis using a single campaign or one year of data can be affected by year-to-year temporal and seasonal shifts, such as annual rain and drought events. A multi-year study can provide a more comprehensive evaluation of the inventories and help us better understand the emission sources in the state.

In this study, we conducted a multiplatform inversion analysis to estimate California annual CH_4 emission estimates for a three-year period from 2014 to 2016, using three different datasets. The study framework optimized statewide CH_4 emissions by adjusting CH_4 surface fluxes from the prior inventory to better simulate observed atmospheric CH_4 mixing ratios. The three different datasets include two tower monitoring networks which provide continuous high temporal quality

data, as well as a series of aircraft measurement campaigns which provide additional spatial coverage to complement the stationary measurements. We conducted six modeling scenarios to conduct a set of analysis and further derived ensemble inversion estimates with 18 ensemble members by combining the six scenarios with the initializations from three different prior inventories to incorporate the uncertainties in the inverse system. It is the first time that such an analysis has been conducted by using multiple measurement platforms and different prior inventories for multiple years to constrain top-down CH_4 emissions in California.

Materials and Methods

Tower- and aircraft-based measurements. This research effort was primarily built around long-term, high quality measurement data collected at a Statewide GHG Monitoring Network operated at multiple regional sites across California by CARB. This network is the first state-operated network of its kind, which provides long-term measurements of atmospheric GHG mixing ratios in California since 2010 with short time intervals (1-5 seconds, depending on site and specific analyzer) and wide spatial coverage (eight towers in the state). The network operates regionally representative monitoring stations throughout the state: two towers in the SV, one in the SFBA, three in the SJV, and two in the SoCAB (Figure 1 and Table S3). All sites of the network conduct continuous ambient air measurements using cavity ring-down CH_4 analyzers with temperature and pressure control (Picarro Inc, Models 1301, 2301 and 2201-i). The systems use permeation tube gas sample driers to dry the intake air and automated drift check and periodic calibration to track accuracy and precision of the instruments. All sites were calibrated with standard reference gases with mixing ratios on the WMO X2004A scale provided by NOAA ERSL's central calibration laboratory[9]. Details about the Statewide GHG Monitoring Network are included in Supporting Information (S1).

We also applied other available research measurements to improve the spatial and temporal resolutions, and better quantify the regional and sectoral distribution of CH_4 emission sources in California. This included airborne and tower-based research measurements which occurred during the same time period (Figure 1), including the Megacities Carbon Project (MCP)[10-12], and NASA's AJAX)[13-14].

The MCP network was started in 2012, and now includes 13 tower/rooftop sites to conduct continuous measurements of CH_4 mixing ratios in the Southern California region. Two of these sites (Mount Wilson (WMO) and San Bernardino (SBC)) belong to the CARB's Statewide GHG Monitoring Network. Three of these sites are considered as the background sites including the San Clemente Island (SCI), Victorville (VIC), and La Jolla (LJO). VIC is deployed mainly to track easterly flow impacted by out of state sources. LJO is located nearby the coast and impacted by on-shore and off-shore flows and potentially provides ocean background information after a precision screening. In this study, we used data from the SCI site as the local background in SoCAB for 2015 and 2016, similar to Yadav et al[12]. To run the inversion analysis, we used data from six of these sites together with CARB sites which were operational during the time period of interest (2015-2016) (Figure 1 and Table S3). We excluded two sites (Granada Hills (GRA) and Irvine (IRV)) in the inversions considering they were greatly influenced by local landfills. Additional inversion studies with GRA and IRV data could be included in future work after careful data screening.

Twelve AJAX flights were deployed and measured CH_4 mixing ratios over the SFBA and the northern SJV during 2013 and 2014. In the study, we focused on the data from six AJAX flights in summer and fall 2014 (15 July, 25 July, 8 October, 15 October, 24 October, and 11 November) (Figure 1). AJAX flights measured CH_4 mixing ratios using cavity ring down spectroscopy (Picarro Inc., model 2301-m) calibrated regularly to NOAA standard gases, and the data were screened for quality and to extract measurements that were taken in or near the planetary boundary layer (PBL) (<2.5 km above ground level). Additional details on the airborne instrumentation and its deployment in the 2014 campaign have been described elsewhere[15-16].

The study analysis focused on tower-based CH_4 measurements obtained during afternoon hours (12-17 Pacific Standard Time (PST)) alone. This was driven by the consideration that the atmospheric boundary layer is well developed during late morning and early afternoon hours, so that the measurements result from surface CH_4 emissions which are then well mixed in the boundary layer. Moreover, the meteorological model generally captures the daytime atmospheric boundary layer, but has difficulty simulating the nocturnal boundary layer after the boundary layer collapse[17]. Therefore, by focusing on the late morning and early afternoon hours, we reduced uncertainties to simulate back-trajectories in the tower receptors for several hours.

We aggregated the hourly tower-based measurements during 12-17 PST into the 3-hour intervals to run the inversions of statewide annual CH_4 emissions for better computational efficiency. We aggregated measurements of airborne-based CH_4 measurements taken from the AJAX field campaign into 30 second intervals for the inversions, similar to Cui et al[18-19] (Figure 2).

Background determination. We used the zonal averaged CH_4 mixing ratios during 2014-2016 between 35º and 43º from NOAA Greenhouse Gas Marine Boundary Layer Reference data[20] to define the backgrounds of CH_4 mixing ratios for the tower sites located outside of the SoCAB and for the aircraft receptors (Figure 2). Measurements from a remote site (Trinidad Head (THD), figure 1) were used to determine the background uncertainty in the inversion analysis. Hourly CH_4 backgrounds determined by measurements at the SCI site (Figure 1) were used for deriving mixing ratio enhancements for tower sites in the SoCAB. The details of hourly background mixing ratios determination in the SoCAB are available in Verhulst et al[10] .We also used the NOAA zonal mean values to determine the background data for 2014 for the two sites (WMO and SBC) in the SoCAB region before MCP network was fully implemented.

Atmospheric transport. CH_4 was treated as a passive atmospheric tracer and the transports of CH_4 from the surface fluxes to the ambient atmosphere was simulated by the FLEXible PARTicle (FLEXPART) Lagrangian particle dispersion model[21] driven by the Weather Research and Forecasting (WRF[22], version 3.7.1) mesoscale model. Back-trajectories from FLEXPART-WRF provided the sensitivities of gridded surface CH_4 fluxes to measured CH_4 mixing ratios, which are called the "footprints" (Text S1). WRF model simulations were conducted with three nested domains at the spatial resolutions of 36km, 12km, and 4km, respectively. The WRF configuration (Text S1) is similar to Cai et al. [23-24], which was used for air pollution simulations in California. To conduct the long-term simulations in WRF, we made the following modifications to the WRF configuration: 1) setting the WRF simulation timescale to a 6-day period, with the 1st day as model spin-up; 2) applying the WRF objective analysis for the outermost domain in the study; 3) using the Pleim-Xiu land-surface model[25-26] to all of WRF domains to improve the first guess fields based on analysis data; 4) turning off the topographic surface wind correction in the innermost domain; 5) modifying the top layer of the vertical structure from 50 hPa to 100 hPa with the same number of the vertical layers; 6) updating sea surface temperature (SST) every 6 hours using time-varying Global Ocean Data Assimilation Experiment High Resolution SST data; and 7) initializing

146 the soil moisture in the Pleim-Xiu land-surface model with surface moisture availability look-up
147 table for April through October, and with analysis data for other months.

148 WRF performance has been evaluated by Cai et al.[24] for vertical distribution of temperature,
149 relative humidity, and wind speed using two-day aircraft measurements in the summer of 2008.
150 Good agreement between model and observations was found near surface. Additionally, the same
151 model configuration was used to simulate ozone in the SJV during May-September 2012[27], and
152 the long-term model simulations captured the meteorology, i.e. wind speed, temperature, and
153 relative humidity, reasonably well based on observations. Here we further evaluate WRF PBLH
154 simulations using PBLH retrievals using available measurements from radiosondes, radar wind
155 profilers, ground-based LiDAR instruments[28], and aircraft soundings during 2014-2016.
156 Additional details are available in Supporting Information (Text S1). The mean biases of simulated
157 PBLH during 12-17 LT were within 13-316 m or 2-65% of the measurement-determined PBLH
158 on average. In addition to model errors, the biases also include the uncertainty from determining
159 PBLH based on these observation platforms.

160 Simulations from the WRF's innermost domain were used to drive FLEXPART and map the
161 footprints to a 0.1 x 0.1-degree spatial resolution consistent with the gridded prior inventories as
162 discussed as below. Each hourly data point from the CARB's Statewide GHG Monitoring Network
163 (2014-2016) and MCP (2015-2016) during 12-17 PST was considered as a receptor. FLEXPART
164 was configured to release 5000 particles at the height of receptors and model the transport of the
165 particles backward in time for 3 days for each receptor of the CARB's Statewide GHG Monitoring
166 Network, and 1 day for each receptor of the MCP. The back-trajectories were also aggregated into
167 the 3-hour intervals for the inversions. For the aircraft measurements, we consider each 30-second
168 averaged data point as a receptor, and we simulated 1-day back-trajectories for each receptor. The
169 duration of backward simulations was chosen based on some sensitivity tests (Text S1).

170 As observed from the footprint analysis, each data platform offers a unique footprint (Text S1).
171 The MCP network focuses on the SoCAB region, and the AJAX flights provided insights in the
172 SFBA and northern SJV regions, while the CARB network provided an overall statewide coverage
173 but has limitations in providing comprehensive regional and local coverage for all source sectors.
174 We ran a variety of cases which combined monitoring data from the different available platforms

and identified the dataset in each region which provided the highest footprint coverage (Table S4). These cases were considered as the optimum regional case and we showed their values independently.

Prior inventories. This study utilized two available gridded CH_4 emission inventories for California for calendar year 2012 as the original prior inventories (Figure S2). The first inventory was obtained from the spatially explicit CALGEM emission model (CALGEM, version 3, 2016), after scaling to match the CARB statewide inventory total by region and emission sector[2]. The second inventory was obtained from a gridded national inventory of U.S. methane emissions[29] which is designed to be consistent with the 2016 edition U.S. Environmental Protection Agency (EPA) inventory of US Greenhouse Gas Emissions and Sinks (GHGI)[30] for the year 2012, from which the emissions data for California region was spatially extracted (hereafter "EPA-GHGI"). Both of these inventories were gridded at 0.1 x 0.1-degree spatial resolution, and the annualized aggregated emissions were extracted for the annual emission analysis in the study. The sectors of wetland and crop agriculture have seasonal variations in CALGEM and the sectors of manure management, natural gas and petroleum production, stationary combustion, and forest fires have monthly/daily variations in EPA-GHGI. However, due to the lack of California-specific seasonal factors for many of the anthropogenic sources, which have been found to have seasonal variation, such as livestock, landfill, and natural gas demand[12, 31-32], we thereby did not configure our inversions to include the temporally varied priors. The overall prior simulations were evaluated and the analysis suggested that observations were underestimated by model prior simulations with absolute mean biases ranging between 24-45 ppb, and the coefficient of determination (R^2) values ranging from 0.3-0.4 (Figure S3).

We also conducted a multivariate analysis by combining the different sector groups from the two inventories in different combinations to construct a hybrid inventory that would provide the additional spatially-resolved prior information. The hybrid inventory which offered the highest R^2 in simulating CH_4 concentration against the observations was chosen ("Hybrid prior") (Text S1). Thereafter, the two original inventories and the third hybrid inventory were used as the prior information to initialize the inverse modeling system, and the posterior estimates were compared against the prior to identify the inversion scenario which showed the most improvement. Since

CARB publishes a statewide total CH_4 emission inventory, we also compared these posterior statewide estimates against the CARB inventory.

Based on the selection of our hybrid inventory, we found the differences between the hybrid inventory and CALGEM were mainly from the dairy livestock (DLS) and the oil and natural gas (ONG) sectors. The optimized hybrid inventory utilized the higher emissions from EPA-GHGI for the DLS and ONG sectors, which are higher than the CALGEM inventory by 19% and 3%, respectively. It should be noted that this analysis does not suggest that the hybrid inventory is the best prior inventory, however, it adds another dimension to reducing the prior inventory uncertainty in the inverse system and can be used to better understand the emission sectors in the region.

Inverse modeling framework. The statewide CH_4 top-down emissions were derived using a mesoscale Bayesian inverse modeling system. This system was consistent with the framework published by Cui et al.[18, 33-34] (Text S1). The study implemented a series of inversion cases to conduct inversion analysis for the statewide total CH_4 emissions during 2014-2016. The descriptions of the inversion cases are shown in Table S7. "2014_Inv", "2015_Inv", and "2016_Inv" were conducted using CH_4 mixing ratio measurements from the CARB's Statewide GHG Monitoring Network. These cases were also useful to investigate the capabilities of the current CARB GHG Monitoring Network to constrain the statewide CH_4 emissions. "2015_Inv_urban" and "2016_Inv_urban" were conducted by adding the MCP monitoring network data in the SoCAB to the CARB's Statewide GHG Monitoring Network data. In addition to estimating the statewide emissions, these two cases were also useful to investigate the utility of a regional intensive urban network in improving the regional CH_4 emission estimates. In addition to the above scenarios, we also tested a case which combined data from the AJAX campaign with the CARB's Statewide GHG Monitoring Network data for calendar year 2014 ("2014_Inv_flight") to investigate the utility of adding aircraft measurements with a large spatial coverage to a regional monitoring network.

Results and discussion

Statewide total CH_4 emission estimates. We conducted multi-platform inversions to derive top-down statewide CH_4 emissions based on the 18 combinations (6 datasets and 3 prior inputs) of measurement networks and a-priori emission inventories during 2014-2016. Figure 3 shows the inversion results from the 18 individual cases, along with ensemble estimates for each year, as well as the overall ensemble estimate for the 2014-2016 period. The maps of differences between the posterior and prior estimates are shown in Figure S10. We also computed the statewide maps related to the Fisher information matrix[18] to investigate the emissions constrained by the observation platforms within the inverse modeling system (Figure S11). The regions associated with high values of the diagonal of Fisher information matrix represent the areas of the domain that are well constrained by the observations. More ensemble estimates are presented in Table S8 from the three types of measurement platform and the three types of prior inventories.

For each case, we compared the CH_4 observations used in the inversions (single platform or multiple platforms) against simulated CH_4 concentrations using the prior inventory and the posterior estimates, respectively (Table S9). R^2 and the mean biases (model minus observation) are used to highlight the improved data-model fit given by the posterior emission estimates. For cases using the tower platforms ("CARB towers", and "CARB towers + MCP towers"), the R^2 are improved from 0.1-0.4 based on the prior inventory to 0.3-0.4 based on the posterior estimates. R^2 values related to the cases of "CARB towers + AJAX flights" fall within the value of ~0.3 using the prior inventory originally and are also slightly improved in the posterior estimates. Moreover, the mean biases in all of cases decreased distinctly using the posterior estimates compared to the cases with the prior inventory in the study as expected.

In Figure 3, we compared the study results against the bottom-up annual CH_4 emission estimates from the CARB inventory for the three years (2014-2016), and showed the range of research emission estimates reported in the literature for statewide CH_4 emissions. We also compiled the annual emission estimates from CALGEM and EPA-GHGI for 2012 for comparison. We calculate the top-down statewide CH_4 emission inventory in California to be 2.05±0.26 Tg/yr (at 95% confidence) based on our 18 different inversions in the study. There is no significant change in statewide CH_4 emission estimates from the CARB inventory during 2014-2016, and the three-year averaged statewide CH_4 emissions were 1.57 Tg/yr. This suggests that the inversion analysis of the CH_4 emissions in California are larger than the CARB inventory by a factor of 1.14-1.47. They

are also higher than CALGEM estimates by a factor of 1.0-1.4, and slightly higher than EPA-GHGI by a factor of 0.9-1.2. Although there are differences in the total emission estimates for the subsets of ensemble analysis, the overall values are consistent within the uncertainty (Figure 3). Previous top-down studies have estimated statewide total CH_4 emissions to be 1.51-3.70 Tg/yr (Table S1), therefore, the emissions estimated in this study fall within the range of previous studies but are on the lower end of the spectrum, and is also consistent with our conservative assumption in the inversion framework setup (see Text S1).

CARB bottom-up CH_4 inventory only focuses on anthropogenic sources, whereas the top-down inversions derive total CH_4 emissions. Emissions from natural sources of CH_4 in California, such as petroleum seeps[35-36] and wetlands[37] could partially contribute to the differences between the bottom-up inventory and top-down estimates. California wetland emissions are estimated to be 0.04 Tg/yr[33], while La Brea Tar Pits (the large petroleum seep) were estimated to be emitting 0.06 Tg/yr[38]. Together with other excluded emissions (0.11 Tg/yr) in the CARB inventory[2] likely contribute 15%-50% of the discrepancies between the CARB inventory and our inversions. In addition, other contributions from "super-emitters"[39-41], episodic emission events[42], other un-inventoried sources, as well as the use of non-region-specific generalized emission factors may be underestimating actual emissions and could contribute to the differences.

There are some differences between the results from cases for the three different platforms (Table S8) in terms of the central value of ensemble results. The change between "CARB towers" and "CARB towers + AJAX flights" due to the addition of the measurements from NASA AJAX flights modifies the emission estimates in Northern California. On the other hand, The estimates from "CARB towers + MCP towers" case present higher total statewide CH_4 emissions compared with the cases of "CARB towers". These differences are primarily driven by changes in CH_4 emission estimates in the SoCAB region where the MCP network was deployed. Additional regional differences are explored in detail in the next sections.

Sub-regional CH_4 emission estimates. This study was able to extract CH_4 emission estimates in the sub-regions to analyze their contributions to the statewide CH_4 emissions in California, using spatially resolved inversion estimates (Figure 4 and Figure S14). In general, our ensemble

inversion estimates in the study by region fall into the range of previous top-down studies. Comparing inversion estimates in the study with the two gridded inventories, we found CH_4 budget estimates from EPA-GHGI and this study are closer in the Central Valley (SJV and SV) than CALGEM, but CALGEM estimates and this study are closer in the SoCAB region. CH_4 emission estimates for SFBA likely are underestimated by the current two bottom-up inventories.

South Coast Air Basin. The footprint values in Table S4 show that the "CARB towers + MCP towers" cases provide additional information to constrain SoCAB emissions beyond the "CARB towers" cases. In the maps calculated by the Fisher information matrix for the SocAB (Figure S11), we also can compare the sensitivity of two tower sites (MWO and SBC) used in the "CARB towers" cases against the sensitivity offered by eight towers used in the "CARB towers + MCP towers" cases. The larger coverage associated with the higher values of the Fisher information matrix in the "CARB towers + MCP towers" cases indicate the importance of the MCP deployment, and CH_4 emissions in SoCAB were better constrained by the addition of data from the MCP platform.

We estimated CH_4 emissions in the SoCAB during 2014-2016 to be 0.39±0.18Tg/yr, which is higher than the corresponding estimates from the CALGEM (0.349 Tg CH_4/yr) by a factor of 0.6-1.6, and higher than EPA-GHGI (0.257 Tg CH_4/yr) by a factor of 0.8-2.2.

The exceptional gas leak event at Aliso Canyon took place during October 2015 to February 2016[42]. A CARB report quantified the CH_4 emissions from the leak event and estimated that 0.0996 Tg CH_4 was emitted into the atmosphere during the event, with 0.0784 Tg CH_4 released in 2015 and 0.0212 Tg CH_4 released in 2016[38]. We estimated the total CH_4 emissions to be 0.36±0.08, 0.42±0.22 and 0.38±0.20 Tg/yr for the years of 2014, 2015, and 2016, respectively. We did not specially exclude the measurements during the event period in the inversions, therefore, the higher estimates for CH_4 emissions in 2015-2016 than the value in 2014 may due to the Aliso Canyon event. The difference of estimates in 2015-2016 against estimates in 2014 is comparable with the contribution of the Aliso Canyon event reported by CARB and Conley et al[42]. This also indicates that top-down studies capture all the emissions from all the sources in a region, including episodic events. Therefore, additional caution and caveats should be considered in direct comparisons

against generalized bottom-up inventories that are not corrected for regions and time periods of interest.

San Joaquin Valley. According to the ensemble inversions, The total CH_4 emissions in the SJV were quantified to be 0.94±0.18 Tg/yr, which is higher than CALGEM (0.78 Tg/yr) by a factor of 1.0-1.4, and higher than EPA-GHGI (0.90 Tg/yr) by a factor of 0.8-1.2. Two independent top-down studies from Jeong et al.[2] and Cui et al.[19] have quantified CH_4 emissions based on tower network and aircraft measurements respectively in the same region, and our results in this study are within the range of previous estimates.

In evaluating the spatial coverage and effective constraints offered by the current monitoring network (Figure S1 and Figure S11), the region with the lowest constraints was observed in the southern SJV, with gaps in Tulare, Kings, Fresno, and Madera counties – all of which contain large agricultural sources. These regions stand out as the highest priority for network expansion in the entire state. Adding additional measurements in SoCAB from MCP did not provide any additional improvement for the SJV domain given the topographical constraints offered by the mountainous region at the confluence of SoCAB and SJV which significantly limit wind flows between the two regions.

Sacramento Valley and San Francisco Bay Area. We also estimated annual CH_4 emissions for the SV and SFBA areas (Figure 4). Based on the ensemble results, we estimated CH_4 emissions in SV to be 0.21±0.04 Tg/yr, which is 1.0-1.5 and 0.7-1.1 times the CALGEM (0.17 Tg/yr) and EPA-GHGI (0.23 Tg/yr) inventories, respectively. Similarly, the ensemble emissions range of CH_4 emissions in SFBA was estimated to be 0.16±0.05 Tg/yr, which is 0.8-1.5 times the corresponding CALGEM (0.14 Tg/yr) and EPA-GHGI (0.14 Tg/yr) inventories. Future work in these areas is necessary, although they are not the largest contributors to the statewide CH_4 emissions.

Overall, the multiplatform inversions of the regional CH_4 emissions are consistent with observed regional "hotspots" by SCIAMACHY satellite[43-44] and an aircraft campaign[45]. The suite of inversions compared with previous studies also supports the robustness of our inverse modeling in conducting spatially resolved analysis.

Temporal variation. We presented the inter-annual and monthly variation of CH_4 emissions based on the posteriors estimates (Figure 3 and Figure S12-S13). First, we did not observe the significant annual variability for the statewide and regional CH_4 emissions during 2014-2016. This flat trend was partly expected, as there weren't any major new regulations or programs in the state during the period of the study, which also were considered in the similar drought condition. For the SoCAB the Aliso Canyon event could explain the enhancements in 2015-2016, especially the year of 2015. The monthly variation of the statewide CH_4 emissions appeared in the posterior estimates, such as the enhanced emissions shown in summer and winter. The enhancements in summer may attribute to the livestock manure mangement and landfills, and the winter enhancements could attribute to the natural gas demand. For the SV, the rice cultivation could explain the enhancements in summer months. The monthly patterns are relatively complicated and unclear in SoCAB, SFBA, and SJV. Nevertheless, it should be noted that the associated large uncertainties degrade the temporal variation analysis. In the study, the current inversion configuration has limitation to inversely resolve the monthly variability of CH_4 emissions due to the static priors, the large model uncertainty, and the limited sensitives of the current GHG monitoring network to some of sources which may have the temporal variation.

Sectoral CH_4 emission estimates. Sectoral emission estimates are very important for accurate emission quantification, robust analysis of emission trends, and effective identification and implementation of mitigation strategies. Although an inversion study encounters substantial challenges in quantifying sectoral emissions due to the uncertainties from the transport model and the prior estimate at such small scales, the processes of inverse modeling studies can provide information to understand sectoral emissions in certain scenarios. For instance, inverse modeling can be used to understand sectoral emissions in sub-regions which have relatively distinct spatial distributions of emission sectors, such as the SJV. Therefore, we further analyzed the data for the SJV to evaluate the sectoral emission distributions in the region. Similar analyses were difficult in SoCAB, SFBA, and SV, where the sectors are collocated within the spatially resolved estimates for the regions.

As the two largest emission source sectors in the SJV, emissions from the dairy sector and the oil and natural gas production subsector were estimated individually in the study. Moreover, these sectors in the SJV are relatively isolated geographically. Cui et al.[19] combined the extra spatial

information of the two major sources with the inversion results to obtain their contributions independently. In this study, we used the same spatial information and the source contribution analysis as Cui et al.[19] to calculate the sectoral CH_4 emissions in the SJV based on our multi-platform inversions.

According to the inversions, we derive the total emissions of the dairy and the production of ONG sectors in the SJV to be 0.44±0.36 and 0.22±0.23 Tg CH_4/yr, respectively (Table S10). Based on the same geographical locations, CH_4 emissions from the dairy and the ONG production subsector are estimated by CALGEM to be 0.66 and 0.05 Tg/yr, while EPA-GHGI estimates them at 0.28 and 0.27 Tg CH_4/yr, respectively. As another source of comparison, we note that the analysis of California ONG emissions by Jeong et al.[46] estimated SJV ONG emissions of 0.17 Tg CH_4/yr, roughly midway between the CARB and EPA-GHGI estimates. The distinct differences in spatial patterns between the two prior inventories account for the large uncertainties in our posterior estimates. Specifically, to evaluate the CARB inventory, we focused on the posterior results against the corresponding prior (CALGEM that is scaled to the CARB inventory), the dairy sector is 100%-115% of the prior, which suggests that emissions from the dairy sector may be underestimated in the CARB inventory, whereas the ONG production subsector is similar to the prior estimates. Overall, the large uncertainties associated with the posterior estimates suggest that the current tower network in the SJV likely limits the sectoral emission analysis.

The sectoral emission estimates have been investigated by a previous study (Cui et al [19]), which used airborne measurements to quantify the emissions of the DLS and ONG sources (103 ±29 and 24±11 Mg CH_4/hr, respectively) for summer 2010. Within the uncertainties, our results for the emissions from the ONG production sector are comparable with Cui et al[33]. We could not directly compare the annual emission rates derived in the study with the values from the short-time aircraft study. Overall, the results emphasize that additional measurements and studies are required for understanding the dairy emission estimates in the SJV.

Implications. Long-term measurements of CH_4 mixing ratios play a significant role in developing a consistent and comprehensive analysis of statewide CH_4 emissions, and in tracking the effectiveness of CH_4 emission reduction strategies. Additionally, top-down studies with robust atmospheric measurements can provide a timely review of real-world inventory trends and the

405 effectiveness of emission reduction measures as we reach climate target years. This study used an
406 inverse modeling analysis approach on a multi-year dataset collected from a first-of-its-kind
407 statewide GHG monitoring network and other complementary datasets to evaluate the statewide
408 and regional methane emissions in California. The data and the analysis were useful to provide an
409 independent broad review of the emission estimates in the state and suggest areas of improvement
410 for emissions research as well as network expansion/optimization. The analysis suggests that the
411 total top-down statewide methane emissions are higher than the bottom up anthropogenic
412 emissions estimates by 14-47%, which is consistent with earlier published results in the
413 literature. Some of this discrepancy is likely due to contributions from natural and biogenic
414 sources that are currently not included in the inventory, since they are out of the scope of
415 regulations. Some additional emissions are expected to be contributions from methane super-
416 emitter point sources, and other episodic events. The points to the need for additional source-
417 specific and sector-specific emissions research to better quantify and inform the bottom-up
418 inventories, including research for better California-specific activity and emission factor
419 information for dairy, landfills, and the oil/gas sector, which needs other top-down measurement-
420 based methods or model-based methods with much finer resolution. Overall, a hybrid spatial
421 inventory with landfill and oil/gas sector emissions from EPA-GHGI and the dairy and other sector
422 emissions from CALGEM provided the best optimized model performance. Regionally, the SJV
423 has the largest concentration of methane emission sources with roughly 50% of the statewide
424 CH4 emissions, followed by the SoCAB, SV and SFBA. The dairy sector is the single largest
425 source in the SJV and is roughly twice as large as the next largest emissions source, the oil and
426 natural gas production subsector. The analysis also identifies the highest priority region to expand
427 the monitoring network, as well as points to additional analytical opportunities to better understand
428 the emission sectors in the state.

429 **Next steps.** CARB has started expanding the GHG monitoring network and plans to add three
430 additional stations in the SJV (Figure S15). CARB is also using the analysis products to add two
431 special monitoring stations in the state, with capabilities to conduct ongoing real-time
432 measurement and analysis of Volatile Organic Compounds and several fluorinated gases. This data
433 is expected to be useful to conduct source apportionment analysis to analyze and track the various
434 GHG emissions source sectors. Additionally, CARB is deploying a statewide ceilometer network

to monitor PBLH to evaluate and improve atmospheric transport model simulation. Similarly, continuing airborne measurements will provide valuable data to estimate GHG emissions at multiple spatial and temporal scales for sub-regions, and will be useful to investigate individual source sectors.

Supporting Information

Additional information about the CARB GHG monitoring network, the WRF configuration, FLEXPART-WRF footprints, inverse modeling framework, PBLH evaluation, simulating time in FLEXPART-WRF, hybrid prior inventory, sectoral analysis for San Joaquin Valley, sub-region CH4 emission estimate, and acknowledgement; Figures S1-S17; Table S1−S10.

Acknowledgment

The authors extend sincere gratitude for the support from numerous researchers at CARB, NASA, NIST, NOAA, LBNL, and other partners (details in Supporting Information). The statements and opinions expressed in this paper are solely the authors' and do not represent the official position of the CARB or other funding agencies.

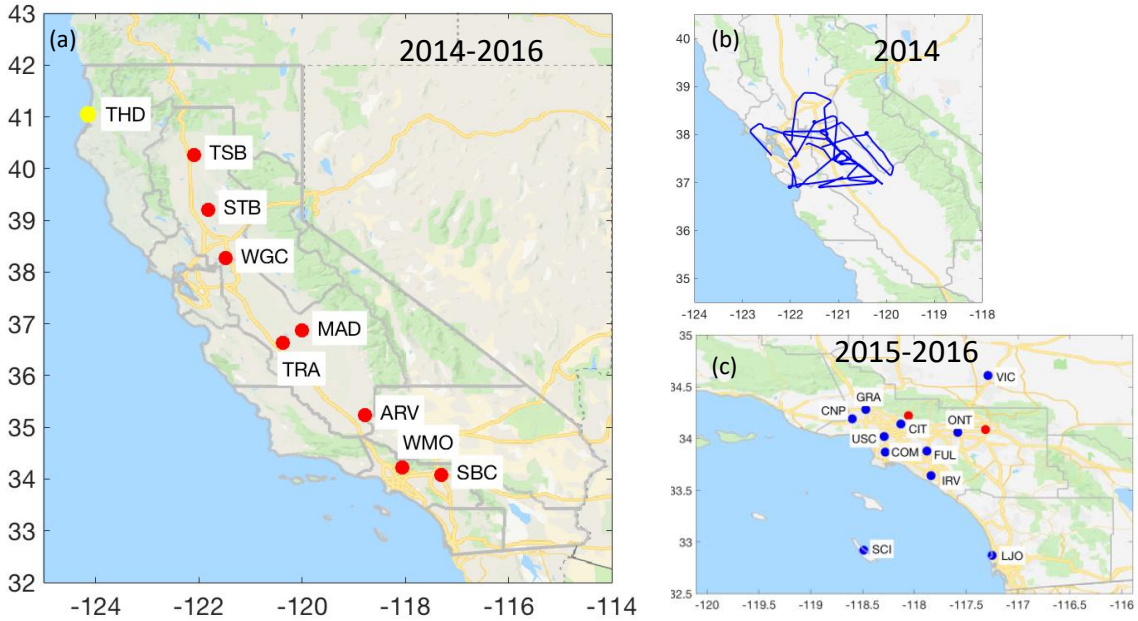

Figure 1. The maps with the locations of the stationary network sites (blue and red dots) and flight path (blue lines) where CH_4 measurements were obtained for the 2014-2016 period.

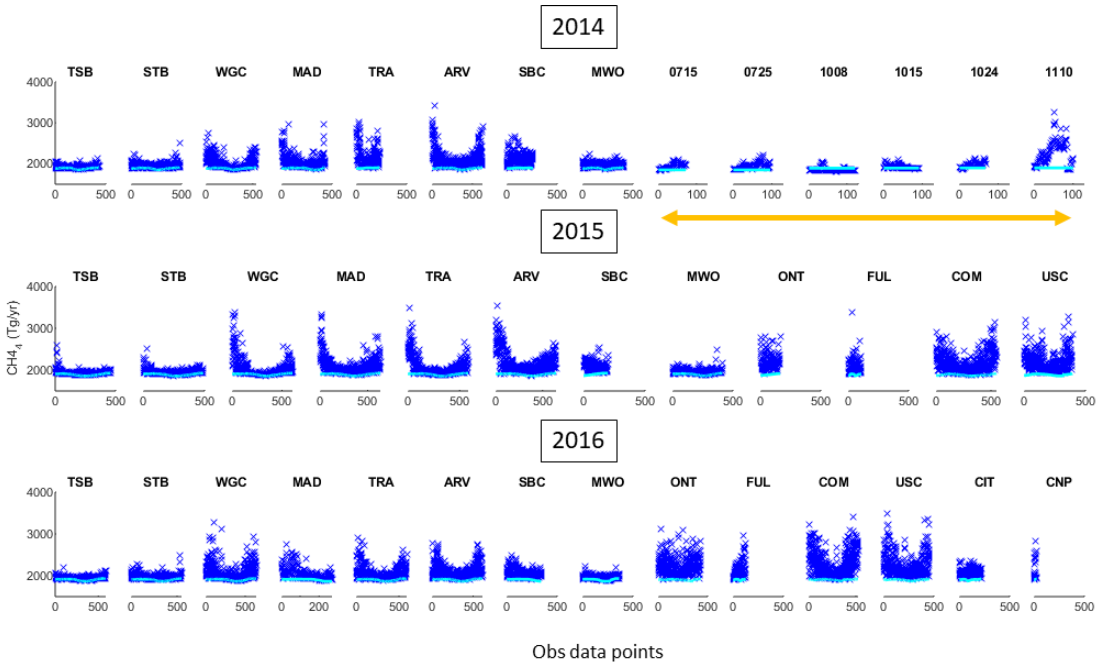

Figure 2. Combined 3-hour averaged CH_4 mixing ratios used in inversions from up to 14 tower sites (blue) and aircraft measurements for 2014-2016 respectively, together with the background values determined in the study (green). Data points marked by the double-headed orange arrow are aircraft measurements.

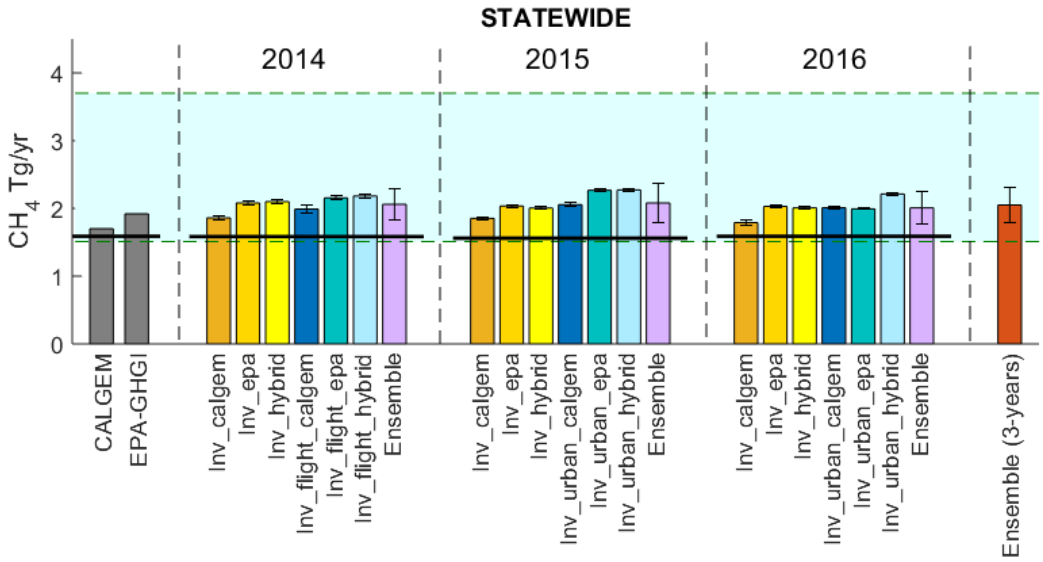

Figure 3. The annual CH_4 emission estimates during 2014-2016 in California derived from this study. The bottom-up inventories (CALGEM version3 and EPA-GHGI) for 2012 are shown as well. The shaded region in light-green represents previous top-down studies listed in Table S1 within the uncertainty analysis (lower and upper bounds are marked as green dashed lines). In addition, the values of black lines are annual CH_4 emission estimates from the CARB inventory. Ensemble values are from 6 members for each year and the 18 members for 3 years. The uncertainty calculated in each inversion case is structured in 1-sigma, and the uncertainties of ensemble results are presented at 95% confidence (2-sigma).

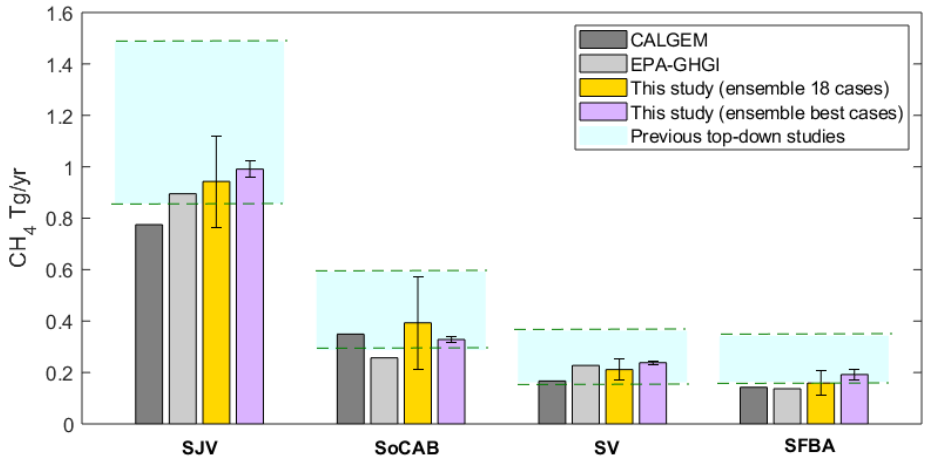

Figure 4. Sub-regional CH_4 emission estimates from our ensemble inversion results of all cases or of cases associated with best footprint coverages, respectively, compared with two gridded bottom-up inventories used in the study. The shaded region in light-green represents previous top-down studies. Inversions in the study include estimates of the exceptional gas leak event at Aliso Canyon. The uncertainties of ensemble results are presented at 95% confidence (2-sigma).

References

1. Wecht, K. J., Jacob, D. J., Sulprizio, M. P., Santoni, G. W., Wofsy, S. C., Parker, R., Bösch, H., and Worden, J., Spatially resolving methane emissions in California: constraints from the CalNex aircraft campaign and from present (GOSAT, TES) and future (TROPOMI, geostationary) satellite observations. *Atmos. Chem. Phys.* **2014,** *14*, 8173-8184.
2. Jeong, S.; Newman, S.; Zhang, J.; Andrews, A. E.; Bianco, L.; Bagley, J.; Cui, X.; Graven, H.; Kim, J.; Salameh, P.; LaFranchi, B. W.; Priest, C.; Campos-Pineda, M.; Novakovskaia, E.; Sloop, C. D.; Michelsen, H. A.; Bambha, R. P.; Weiss, R. F.; Keeling, R.; Fischer, M. L., Estimating methane emissions in California's urban and rural regions using multitower observations. *Journal of Geophysical Research: Atmospheres* **2016,** *121* (21), 13,031-13,049.
3. Kuwayama, T.; Charrier-Klobas, J. G.; Chen, Y.; Vizenor, N. M.; Blake, D. R.; Pongetti, T.; Conley, S. A.; Sander, S. P.; Croes, B.; Herner, J. D., Source Apportionment of Ambient Methane Enhancements in Los Angeles, California, To Evaluate Emission Inventory Estimates. *Environ Sci Technol* **2019,** *53* (6), 2961-2970.
4. Wong, K. W.; Fu, D.; Pongetti, T. J.; Newman, S.; Kort, E. A.; Duren, R.; Hsu, Y.-K.; Miller, C. E.; Yung, Y. L.; Sander, S. P., Mapping CH4 : CO2 ratios in Los Angeles with CLARS-FTS from Mount Wilson. *Atmospheric Chemistry and Physics* **2015,** *15*, 241-252.
5. Wennberg, P. O.; Mui, W.; Wunch, D.; Kort, E. A.; Blake, D. R.; Atlas, E. L.; Santoni, G. W.; Wofsy, S. C.; Diskin, G. S.; Jeong, S.; Fischer, M. L., On the sources of methane to the Los Angeles atmosphere. *Environ Sci Technol* **2012,** *46* (17), 9282-9.
6. Fairley, D., M. L. Fischer Top-down methane emissions estimates for the San Francisco Bay Area from 1990 to 2012. *Atmos.Environ* **2015**, 9-15.
7. Hedelius, J. K.; Liu, J.; Oda, T.; Maksyutov, S.; Roehl, C. M.; Iraci, L. T.; Podolske, J. R.; Hillyard, P. W.; Liang, J.; Gurney, K. R.; Wunch, D.; Wennberg, P. O., Southern California megacity CO2, CH4, and CO flux estimates using ground- and space-based remote sensing and a Lagrangian model. *Atmos. Chem. Phys.* **2018,** *18*, 16271-16291.
8. Wunch, D.; Toon, G. C.; Hedelius, J. K.; Vizenor, N.; Roehl, C. M.; Saad, K. M.; Blavier, J.-F. L.; Blake, D. R.; Wennberg, P. O., Quantifying the loss of processed natural gas within California's South Coast Air Basin using long-term measurements of ethane and methane. *Atmospheric Chemistry and Physics* **2016,** *16*, 14091-14105.
9. Dlugokencky, E. J., R. C. Myers, P. M. Lang, K. A. Masarie, A. M. Crotwell, K. W. Thoning, B. D. Hall, J. W. Elkins, and L. P. Steele Conversion of NOAA atmospheric dry air CH4 mole fractions to a gravimetrically prepared standard scale. *J. Geophys. Res.* **2005,** *110*.
10. Verhulst, K. R.; Karion, A.; Kim, J.; Salameh, P. K.; Keeling, R. F.; Newman, S.; Miller, J.; Sloop, C.; Pongetti, T.; Rao, P.; Wong, C.; Hopkins, F. M.; Yadav, V.; Weiss, R. F.; Duren, R. M.; Miller, C. E., Carbon dioxide and methane measurements from the Los Angeles Megacity Carbon Project – Part 1: calibration, urban enhancements, and uncertainty estimates. *Atmos. Chem. Phys.* **2017,** *17* (13), 8313-8341.
11. Ware, J., Kort, E.A., Duren, R., Mueller, K.L., Verhulst, K.R., and Yadav, V., Detecting Urban Emissions Changes and Events with a Near-Real-Time-Capable Inversion System. *Journal of Geophysical Research: Atmospheres* **2019,** *124*.
12. Yadav, V.; Duren, R.; Mueller, K.; Verhulst, K. R.; Nehrkorn, T.; Kim, J.; Weiss, R. F.; Keeling, R.; Sander, S.; Fischer, M. L.; Newman, S.; Falk, M.; Kuwayama, T.; Hopkins, F.; Rafiq,

T.; Whetstone, J.; Miller, C., Spatio-temporally Resolved Methane Fluxes From the Los Angeles Megacity. *Journal of Geophysical Research: Atmospheres* **2019,** *124* (9), 5131-5148.
13. Yates, E. L., L. T. Iraci, M. C. Roby, R. B. Pierce, M. S. Johnson, P. J. Reddy, J. M. Tadić, M. Loewenstein, and W. Gore, Airborne observations and modeling of springtime stratosphere-to-troposphere transport over California. *Atmos. Chem. Phys.* **2013,** *13*.
14. Hamill, P., Iraci, L. T., Yates, E. L., Gore, W., Bui, T. P., Tanaka, T. and Loewenstein, M. , A new instrumented airborne platform for atmospheric research. *Bulletin of the American Meteorological Society* **2016,** *97*.
15. Johnson, M. S., X. Xi, S. Jeong, E. L. Yates, L. T. Iraci, T. Tanaka, M. Loewenstein, J. Tadic, and M. L. Fischer Investigating seasonal methane emissions in Northern California using airborne measurements and inverse modeling. *J. Geophys. Res. Atmos.* **2016,** *121*.
16. Tanaka, T., E. Yates, L. T. Iraci, M. S. Johnson, W. Gore, J. M. Tadic, M. Loewenstein A. Kuze, C. Frankenberg, A. Butz, and Y. Yoshida, Two-Year Comparison of Airborne Measurements of CO2 and CH4 With GOSAT at Railroad Valley, Nevada. *IEEE Trans. Geosci. Remote Sens* **2016,** *54*.
17. Hu, X., J.W. Nielsen-Gammon, and F. Zhang, Evaluation of Three Planetary Boundary Layer Schemes in the WRF Model. *J. Appl. Meteor. Climatol.* **2010,** *49*.
18. Cui, Y. Y.; Brioude, J.; McKeen, S. A.; Angevine, W. M.; Kim, S.-W.; Frost, G. J.; Ahmadov, R.; Peischl, J.; Bousserez, N.; Liu, Z.; Ryerson, T. B.; Wofsy, S. C.; Santoni, G. W.; Kort, E. A.; Fischer, M. L.; Trainer, M., Top-down estimate of methane emissions in California using a mesoscale inverse modeling technique: The South Coast Air Basin. *Journal of Geophysical Research: Atmospheres* **2015,** *120* (13), 6698-6711.
19. Cui, Y. Y.; Brioude, J.; Angevine, W. M.; Peischl, J.; McKeen, S. A.; Kim, S.-W.; Neuman, J. A.; Henze, D. K.; Bousserez, N.; Fischer, M. L.; Jeong, S.; Michelsen, H. A.; Bambha, R. P.; Liu, Z.; Santoni, G. W.; Daube, B. C.; Kort, E. A.; Frost, G. J.; Ryerson, T. B.; Wofsy, S. C.; Trainer, M., Top-down estimate of methane emissions in California using a mesoscale inverse modeling technique: The San Joaquin Valley. *Journal of Geophysical Research: Atmospheres* **2017,** *122* (6), 3686-3699.
20. https://www.esrl.noaa.gov/gmd/ccgg/mbl/.
21. Brioude, J.; Arnold, D.; Stohl, A.; Cassiani, M.; Morton, D.; Seibert, P.; Angevine, W.; Evan, S.; Dingwell, A.; Fast, J. D.; Easter, R. C.; Pisso, I.; Burkhart, J.; Wotawa, G., The Lagrangian particle dispersion model FLEXPART-WRF version 3.1. *Geosci. Model Dev.* **2013,** *6* (6), 1889-1904.
22. Skamarock, W. C., and Coauthors, A Description of the Advanced Research WRF Version 3. *NCAR Technical Note NCAR/TN-475+STR* **2008**.
23. Cai, C.; Avise, J.; Kaduwela, A.; DaMassa, J.; Warneke, C.; Gilman, J. B.; Kuster, W.; de Gouw, J.; Volkamer, R.; Stevens, P.; Lefer, B.; Holloway, J. S.; Pollack, I. B.; Ryerson, T.; Atlas, E.; Blake, D.; Rappenglueck, B.; Brown, S. S.; Dube, W. P., Simulating the Weekly Cycle of NOx-VOC-HOx-O3 Photochemical System in the South Coast of California During CalNex-2010 Campaign. *Journal of Geophysical Research: Atmospheres* **2019,** *124* (6), 3532-3555.
24. Cai, C.; Kulkarni, S.; Zhao, Z.; Kaduwela, A. P.; Avise, J. C.; DaMassa, J. A.; Singh, H. B.; Weinheimer, A. J.; Cohen, R. C.; Diskin, G. S.; Wennberg, P.; Dibb, J. E.; Huey, G.; Wisthaler, A.; Jimenez, J. L.; Cubison, M. J., Simulating reactive nitrogen, carbon monoxide, and ozone in California during ARCTAS-CARB 2008 with high wildfire activity. *Atmospheric Environment* **2016,** *128*, 28-44.

25. Xiu, A., and J. E. Pleim, Development of a land surface model. Part I: Application in a mesoscale meteorological model. *J. Appl. Meteor. Climatol.* **2001,** *40*.
26. Xiu, P. J. E. a. A., Development of a land-surface model. Part II: Data assimilation. . *J. Appl. Meteor. Climatol.* **2003,** *42*.
27. http://valleyair.org/Air_Quality_Plans/Ozone-Plan-2016.htm.
28. Ware, J.; Kort, E. A.; DeCola, P.; Duren, R., Aerosol lidar observations of atmospheric mixing in Los Angeles: Climatology and implications for greenhouse gas observations. *J Geophys Res Atmos* **2016,** *121* (16), 9862-9878.
29. Maasakkers, J. D.; Jacob, D. J.; Sulprizio, M. P.; Turner, A. J.; Weitz, M.; Wirth, T.; Hight, C.; DeFigueiredo, M.; Desai, M.; Schmeltz, R.; Hockstad, L.; Bloom, A. A.; Bowman, K. W.; Jeong, S.; Fischer, M. L., Gridded National Inventory of U.S. Methane Emissions. *Environmental Science & Technology* **2016,** *50* (23), 13123-13133.
30. https://www.epa.gov/ghgemissions/inventory-us-greenhouse-gas-emissions-and-sinks.
31. Arndt, C.; Leytem, A. B.; Hristov, A. N.; Zavala-Araiza, D.; Cativiela, J. P.; Conley, S.; Daube, C.; Faloona, I.; Herndon, S. C., Short-term methane emissions from 2 dairy farms in California estimated by different measurement techniques and US Environmental Protection Agency inventory methodology: A case study. *Journal of Dairy Science* **2018,** *101* (12), 11461-11479.
32. Spokas, K.; Bogner, J.; Chanton, J., A process-based inventory model for landfill CH4 emissions inclusive of seasonal soil microclimate and CH4 oxidation. *Journal of Geophysical Research: Biogeosciences* **2011,** *116* (G4).
33. Bagley, J. E.; Jeong, S.; Cui, X.; Newman, S.; Zhang, J.; Priest, C.; Campos-Pineda, M.; Andrews, A. E.; Bianco, L.; Lloyd, M.; Lareau, N.; Clements, C.; Fischer, M. L., Assessment of an atmospheric transport model for annual inverse estimates of California greenhouse gas emissions. *Journal of Geophysical Research: Atmospheres* **2017,** *122* (3), 1901-1918.
34. Cui, Y. Y.; Henze, D. K.; Brioude, J.; Angevine, W. M.; Liu, Z.; Bousserez, N.; Guerrette, J.; McKeen, S. A.; Peischl, J.; Yuan, B.; Ryerson, T.; Frost, G.; Trainer, M., Inversion Estimates of Lognormally Distributed Methane Emission Rates From the Haynesville-Bossier Oil and Gas Production Region Using Airborne Measurements. *Journal of Geophysical Research: Atmospheres* **2019,** *124* (6), 3520-3531.
35. Etiope, G., Lassey, K. R., Klusman, R. W. & Boschi, E. , Reappraisal of the fossil methane budget and related emission from geologic sources. *Geophys. Res. Lett.* **2008,** *35*, L09307.
36. Etiope, G., Doezema, L. A., & Pacheco, C. , Emission of methane and heavier alkanes from the La Brea Tar Pits seepage area, Los Angeles. *Journal of Geophysical Research: Atmospheres* **2017,** *122*.
37. He, S.; Malfatti, S. A.; McFarland, J. W.; Anderson, F. E.; Pati, A.; Huntemann, M.; Tremblay, J.; Glavina del Rio, T.; Waldrop, M. P.; Windham-Myers, L.; Tringe, S. G., Patterns in wetland microbial community composition and functional gene repertoire associated with methane emissions. *MBio* **2015,** *6* (3), e00066-15.
38. Jeong, S.; Hsu, Y.-K.; Andrews, A. E.; Bianco, L.; Vaca, P.; Wilczak, J. M.; Fischer, M. L., A multitower measurement network estimate of California's methane emissions. *Journal of Geophysical Research: Atmospheres* **2013,** *118* (19), 11,339-11,351.
39. Introduction to the Phase I Report of the California Methane Survey from the Staff of the California Air Resources Board (CARB). **2017**.
40. Brandt, A. R.; Heath, G. A.; Kort, E. A.; O'Sullivan, F.; Petron, G.; Jordaan, S. M.; Tans, P.; Wilcox, J.; Gopstein, A. M.; Arent, D.; Wofsy, S.; Brown, N. J.; Bradley, R.; Stucky, G. D.;

Eardley, D.; Harriss, R., Energy and environment. Methane leaks from North American natural gas systems. *Science* **2014,** *343* (6172), 733-5.
41. Alvarez, R. A.; Zavala-Araiza, D.; Lyon, D. R.; Allen, D. T.; Barkley, Z. R.; Brandt, A. R.; Davis, K. J.; Herndon, S. C.; Jacob, D. J.; Karion, A.; Kort, E. A.; Lamb, B. K.; Lauvaux, T.; Maasakkers, J. D.; Marchese, A. J.; Omara, M.; Pacala, S. W.; Peischl, J.; Robinson, A. L.; Shepson, P. B.; Sweeney, C.; Townsend-Small, A.; Wofsy, S. C.; Hamburg, S. P., Assessment of methane emissions from the U.S. oil and gas supply chain. *Science* **2018,** *361* (6398), 186-188.
42. Conley, S.; Franco, G.; Faloona, I.; Blake, D. R.; Peischl, J.; Ryerson, T. B., Methane emissions from the 2015 Aliso Canyon blowout in Los Angeles, CA. *Science* **2016,** *351* (6279), 1317-1320.
43. Kort, E. A.; Frankenberg, C.; Costigan, K. R.; Lindenmaier, R.; Dubey, M. K.; Wunch, D., Four corners: The largest US methane anomaly viewed from space. *Geophysical Research Letters* **2014,** *41* (19), 6898-6903.
44. Buchwitz, M.; Schneising, O.; Reuter, M.; Heymann, J.; Krautwurst, S.; Bovensmann, H.; Burrows, J. P.; Boesch, H.; Parker, R. J.; Somkuti, P.; Detmers, R. G.; Hasekamp, O. P.; Aben, I.; Butz, A.; Frankenberg, C.; Turner, A. J., Satellite-derived methane hotspot emission estimates using a fast data-driven method. *Atmos. Chem. Phys.* **2017,** *17* (9), 5751-5774.
45. Peischl, J.; Ryerson, T. B.; Holloway, J. S.; Trainer, M.; Andrews, A. E.; Atlas, E. L.; Blake, D. R.; Daube, B. C.; Dlugokencky, E. J.; Fischer, M. L.; Goldstein, A. H.; Guha, A.; Karl, T.; Kofler, J.; Kosciuch, E.; Misztal, P. K.; Perring, A. E.; Pollack, I. B.; Santoni, G. W.; Schwarz, J. P.; Spackman, J. R.; Wofsy, S. C.; Parrish, D. D., Airborne observations of methane emissions from rice cultivation in the Sacramento Valley of California. *Journal of Geophysical Research: Atmospheres* **2012,** *117* (D24).
46. Jeong, S., D. Millstein and M. L. Fischer Spatially Explicit Methane Emissions from Petroleum Production and the Natural Gas System in California. *Environmental Science & Technology* **2014,** *48*.